



Improving wear resistance and corrosion resistance of AZ31 magnesium alloy by DLC/AlN/Al coating

Guosong Wu^{*}, Wei Dai, He Zheng, Aiying Wang^{*}

Ningbo Institute of Materials Technology and Engineering, Chinese Academy of Sciences, Ningbo 315201, China

ARTICLE INFO

Article history:

Received 21 May 2010

Accepted in revised form 24 August 2010

Available online 16 September 2010

Keywords:

Magnesium alloy

DLC

Ion beam deposition

Sputtering

Wear

Corrosion

ABSTRACT

A novel protective coating, consisting of three layers (top: diamond-like carbon, middle: aluminum nitride, bottom: aluminum), was deposited on the surface of AZ31 magnesium alloy layer by layer. Nano-indenter, electrochemical system and tribological tester were performed to investigate the hardness, wear resistance and corrosion resistance of the coated AZ31 magnesium alloy, respectively. The DLC/AlN/Al coating improved the magnesium alloy's surface hardness and reduced its friction coefficient, which consequently induced a great improvement of the magnesium alloy's wear resistance. Furthermore, the corrosion resistance of the AZ31 magnesium alloy with the DLC/AlN/Al coating was also enhanced with the corrosion current density decreasing from 2.25×10^{-5} A/cm² to 1.28×10^{-6} A/cm² in a 3.5 wt.% NaCl solution.

© 2010 Elsevier B.V. All rights reserved.

1. Introduction

Poor wear resistance and poor corrosion resistance are two main factors to hinder magnesium alloys' widespread use in many applications, particularly outdoor application. One of the most effective ways to avoid wear and prevent corrosion is to coat the magnesium alloys [1]. Now, hard coatings are playing an important role in the protection of magnesium alloys. For instance, TiN, CrN and TiAlN coatings deposited on magnesium alloys by the physical vapor deposition (PVD) technique could effectively improve their surface hardness and wear resistance [2–6]. But, in contrast to the significantly improved hardness and wear resistance, only moderate or some degree of corrosion protection for the substrates was provided mainly due to a large potential difference between electrically-conductive hard coatings (such as TiN) and magnesium alloy substrates. This is because galvanic corrosion always arises in the thickness-through defects of the coatings in corrosive media with the formation of a circuit for current to occur from the more active Mg alloy substrate to the more noble hard electrically-conductive coating. The anodized coating of magnesium alloy, which consists mainly of magnesium oxide, is also one of typical hard coatings. Compared to those conductive hard coatings, it is insulative and not easy to form strong galvanic corrosion in corrosive media. But, its porous structure becomes a key factor to easily induce local corrosion [7–9].

Except for these above hard coatings, diamond-like carbon (DLC) is a good alternative to act as the protective coating because it owns a

high mechanical hardness, a chemical inertness and a dense microstructure [10]. In recent years, some researchers have attempted to apply it to improve the mechanical property and anti-corrosion property of magnesium alloys [11–14]. However, it is generally believed that hard materials, such as DLC coatings, are hard to be directly deposited onto soft substrates, such as magnesium alloys, due to the large difference in physical properties between them (e.g. elastic modulus, plasticity and thermal coefficient of expansion) [15,16].

To relieve the influence of the physical properties difference between DLC coating and Mg–Li alloy substrate, Si layer was used as a buffer in the study [11]. Unfortunately, both the adhesion and the corrosion resistance of the coated sample were not improved in the artificial perspiration. In our previous work [16], Cr and CrN were also selected as interlayers in the DLC coating/AZ31 magnesium alloy system. Although the adhesion was greatly improved with the addition of these interlayers, the corrosion resistance in the 3.5 wt.% NaCl solution was not enhanced due to the formation of galvanic cells between substrate and interlayer in the through-thickness defects.

According to the above research results, another material should be reconsidered for acting as the interlayer to reduce the effect of galvanic corrosion. In theory, aluminum will reduce the galvanic corrosion to a relatively great extent because the electrode potential of aluminum is nearer to that of Mg alloys in contrast to chromium [17]. Pardo et al. have ever prepared thermal sprayed aluminum coatings on Mg–Al alloys and found that the corrosion resistance of the coated alloys was significantly improved [18]. Wu et al. attempted to use sputtering to deposit Al films on AZ31 magnesium alloys and also proved that the sputtered Al film could enhance the corrosion resistance of magnesium alloy [19]. Thus, it seems that Al film as an interlayer is more effective than Cr film based on the electrochemical

^{*} Corresponding authors. Tel./fax: +86 57486685036.

E-mail addresses: guosonwu@cityu.edu.hk, wugsjd@126.com (G. Wu), aywang@nimte.ac.cn (A. Wang).

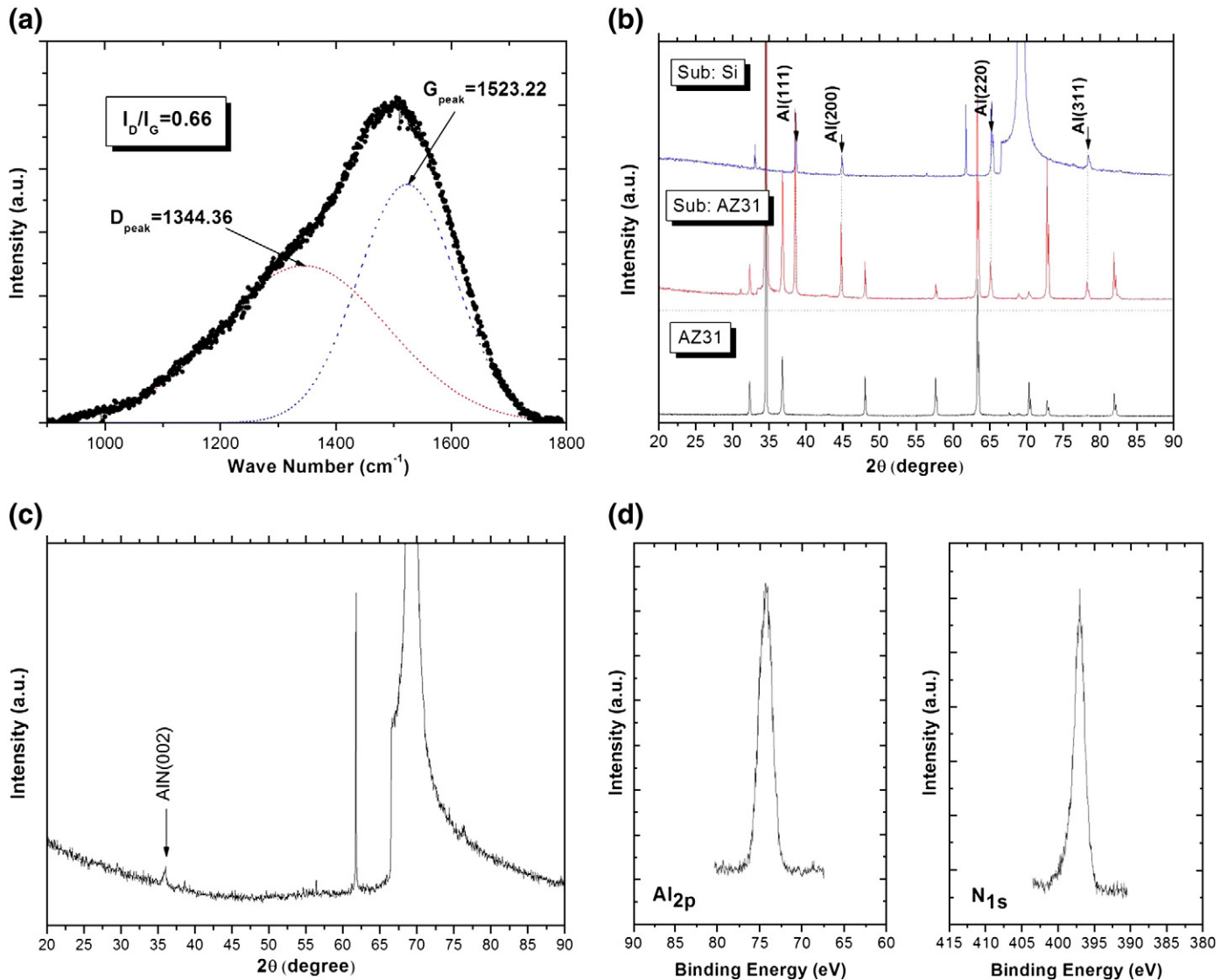


Fig. 1. (a) Raman spectra of the diamond-like carbon film, (b) XRD pattern of the aluminum film, (c) XRD pattern of the aluminum nitride film and (d) high resolution XPS spectra of the aluminum nitride film.

theory. Nevertheless, the load-bearing capacity has to be considered because Al film is also a very soft metal in contrast to the DLC film. In the study of Altun et al. [20], an Al interlayer was deposited onto the Mg alloy substrate before the AlN coating, which induced good adhesion and good corrosion resistance. Therefore, AlN/Al as an interlayer seems to be a possible choice to not only reduce the effect of galvanic corrosion but also hold the load-bearing capacity. In this study, we attempted to add the AlN/Al film as a combined buffer layer into the system of the DLC coating/AZ31 magnesium alloy substrate and subsequently investigated the wear resistance and corrosion resistance of the coated magnesium alloy.

2. Experimental

2.1. Sample preparation

As-extruded AZ31(Mg-3 wt.%Al-1 wt.%Zn) magnesium alloy plates were ground with emery paper up to 1500 #, polished with Al₂O₃ paste (average size 100 nm), and then ultrasonically washed in ethanol (analytical reagent) for 5 min. A hybrid ion beam deposition system (including a linear ion source and a magnetron sputtering source) as shown in the literature [21] was used to prepare protective

coatings on AZ31 plates. The protective coating was designed as a three-layer structure, aluminum layer, aluminum nitride layer and diamond-like carbon layer stacked by turns from the bottom to the top.

In the preparation process, the ion source with Ar gas was first applied to etch the substrate for 10 min when the base pressure of the chamber was below 2×10^{-5} Torr. Next, the magnetron sputtering source with an Al (99.99%) target was used to prepare the AlN/Al interlayer with Ar as sputtering gas and N₂ as reactive gas. Last, the linear ion source was used to prepare the diamond-like carbon coating with C₂H₂ as the source gas.

As described above, the coating process was divided into three stages. In the first stage, the Al layer was deposited onto the magnesium alloy substrate with a sputtering current of 2 A, an Ar flux of 40 sccm, and a deposition time of 30 min. In the second stage, the AlN layer was deposited onto the surface of the Al layer with a sputtering current of 2 A, an Ar flux of 40 sccm, a N₂ flux of 40 sccm, and a deposition time of 30 min. In the third stage, the DLC film was deposited on the surface of the AlN layer with an ion source current of 0.2 A, a C₂H₂ flux of 40 sccm, and a deposition time of 30 min. The chamber temperatures and chamber pressures were about 35 °C and 2.2×10^{-3} Torr at the first stage (Al sputtering), 35 °C and 4.1×10^{-3} Torr at the second stage (AlN

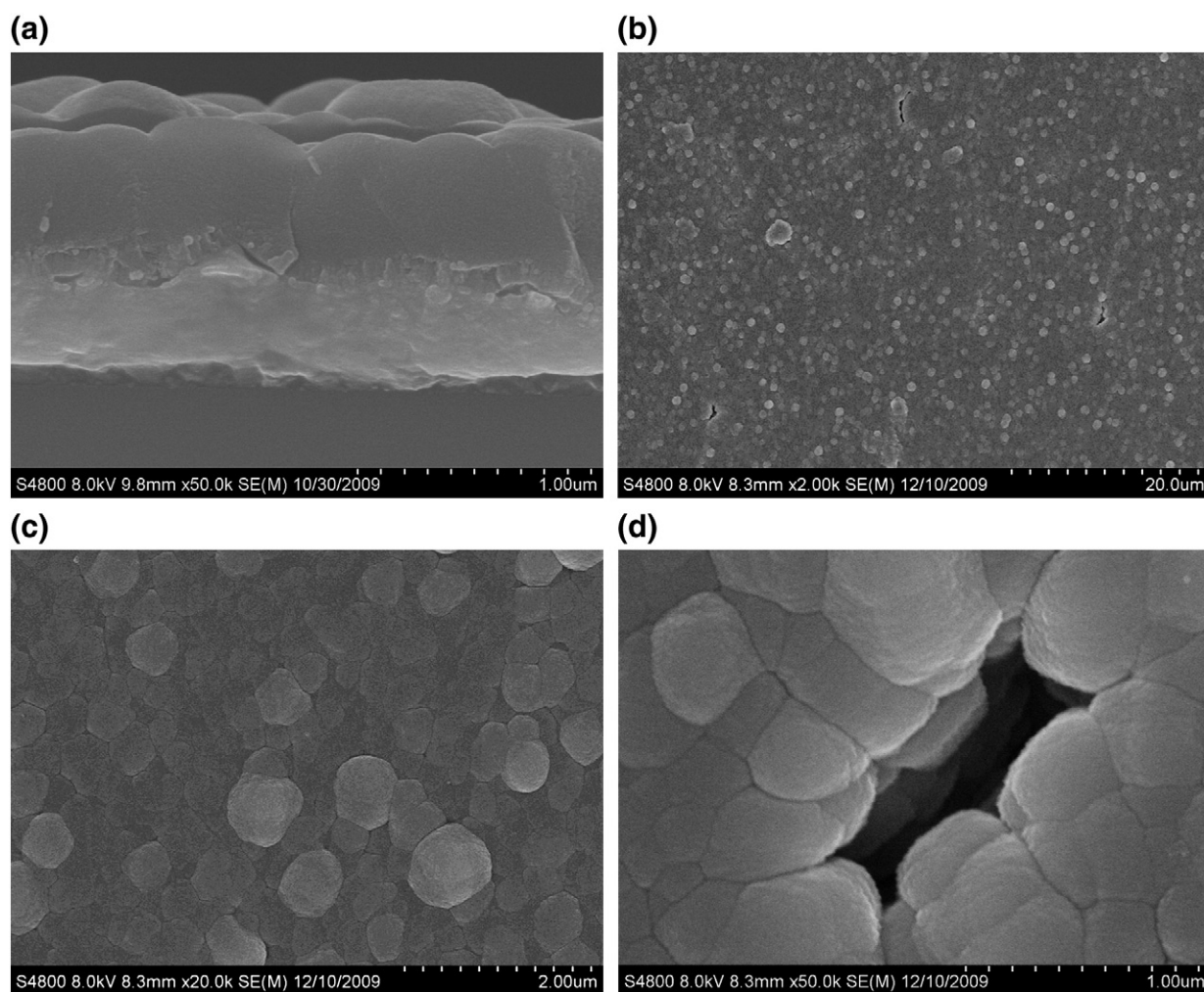


Fig. 2. SEM micrographs of the prepared coating: (a) cross section of the coating deposited on Si substrate (b), (c) and (d) surface morphology of the coating observed at different magnifications.

sputtering) and 80 °C and 1.2×10^{-3} Torr at the third stage (DLC deposition), respectively. In all stages of the coating process, the substrate rotated at a speed of 4.2 rpm. Bias voltage was set as -100 V and applied at pulse mode with a frequency of 350 kHz.

2.2. Coating characterization

Field emission scanning electron microscope (FESEM) was performed to characterize the cross section and surface morphology of the obtained coatings. X-ray diffraction meter with Cu K α radiation was used to study the crystal structure of the obtained coatings. Raman spectroscopy with an incident Ar⁺ at a wavelength of 514.5 nm was used to measure the atomic bonds of DLC films. An X-ray photoelectron spectroscopy (XPS) with Al (mono) K α irradiation at a pass energy of 160 eV was used to characterize the chemical bonds of the films. The binding energies were referenced to the C 1s line at 285.0 eV.

2.3. Property testing

The tribological behaviors of the treated sample was measured on a rotary ball-on-disk tribometer at room temperature with a relative humidity of 40–50% under dry sliding conditions. A SiC ball with a diameter of 7 mm was used as the friction counter body. All the tests were performed at a sliding speed of 50 mm s⁻¹ and the applied load was 1 N. After the tribological test, the wear tracks were investigated

by a surface profiler and optical microscope (OM). A MTS nano-indenter was performed to test the hardness and elastic modulus of the treated samples in this study.

For the electrochemical investigation, the experiments were controlled by an AUTOLAB PGSTAT302 advanced electrochemical system at room temperature, using the conventional three-electrode technique. The potential was referred to a saturated calomel electrode (SCE) and the counter electrode was a platinum sheet. Each sample was masked by paraffin waxes with a surface area of 1×1 cm² exposed in the 3.5 wt.% NaCl solution. The potential was scanned from the cathodic region to the anodic region with a scan rate of 1 mV/s. Salt immersion test (3.5 wt.% NaCl solution) was further used to investigate the corrosion resistance of the coated sample.

3. Results and discussion

3.1. Coating characteristics

In order to characterize the DLC/AlN/Al coating, DLC film, AlN film and Al film were prepared under the same deposition condition as their corresponding layer in the multilayer structure. Fig. 1(a) shows the Raman spectra of the diamond-like carbon film, which can be deconvoluted into two sub-peaks: G band at 1523.22 cm⁻¹ and D band at 1344.36 cm⁻¹. According to this typical pattern, it means that the DLC film has been successfully obtained by the ion beam technique. Diamond-like carbon mainly contains sp³ bond and sp²

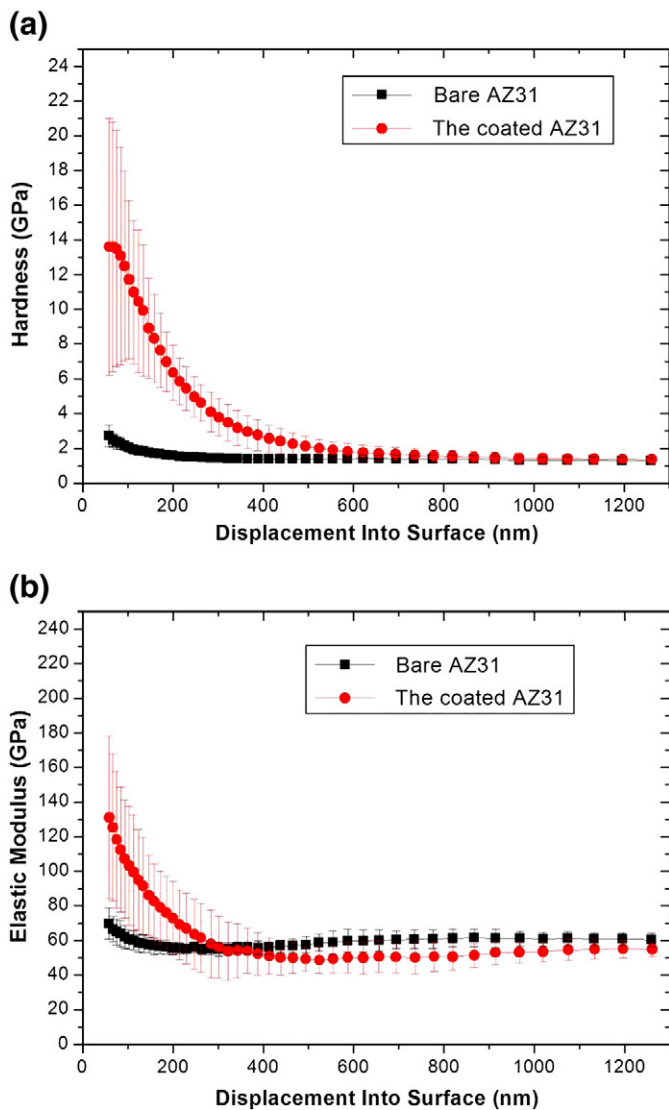


Fig. 3. Hardness (a) and elastic modulus (b) of the samples as a function of displacement.

bond, but visible Raman spectroscopy is only sensitive to sp^2 sites. In the Raman spectra, G means a graphite structure and D means a disordered graphite-like structure, not a diamond structure. The presence of D band is attributed to the bond-angle disorder in the graphite structure induced by the linking with sp^3 carbon atoms and to the lack of long distance order in graphite-like microdomains [22]. In general, a shift of G band to lower wave numbers with a decreasing of the I_D/I_G ratio means an increase in the fraction of sp^3 bonds [23,24]. The I_D/I_G value shown in Fig. 1(a) is only 0.66 and the position of G peak is lower than the typical range of 1540–1580 cm^{-1} , so it suggests that this DLC film owns a sp^3 rich microstructure. Fig. 1(b) gives the XRD patterns of the Al layer on the silicon substrate and AZ31 substrate. Deducting the signals of Si and AZ31 substrates from XRD patterns, it is easily identified that the four peaks are corresponding to Al (111), Al (200), Al (220) and Al (311). Fig. 1(c) shows the XRD patterns of the AlN layer deposited on the silicon substrate. According to the research results of other scholars [25,26], it is found that this AlN coating presents the (002) preferred texture. The high resolution Al_{2p} and N_{1s} XPS spectra of the aluminum nitride film are given in Fig. 1(d). According to the literatures [27,28], both the Al_{2p} peak centered at 74.2 eV and the N_{1s} peak centered at 397.0 eV are corresponding to the Al–N bond of aluminum nitride. In a word, it can

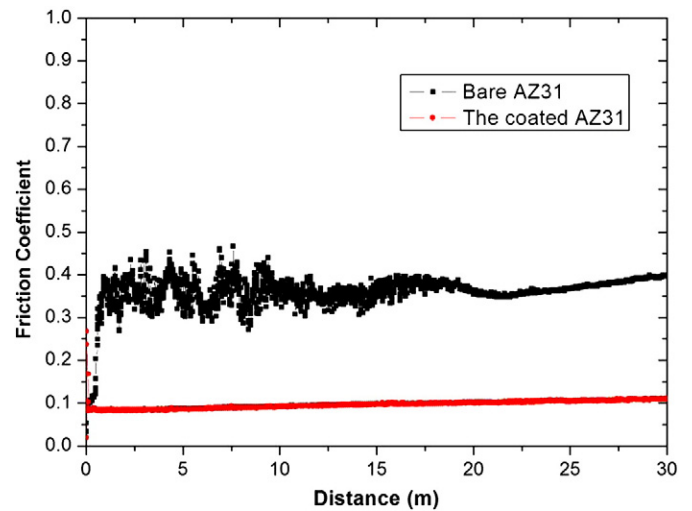


Fig. 4. Friction coefficient of the samples vs. sliding distance.

be concluded from these above characterizations that the DLC/AlN/Al three-layer structure has been successfully obtained in this study.

The cross section of the DLC/AlN/Al coating is shown in Fig. 2(a). It is known that magnesium alloy substrate is very hard to be split compared to other brittle materials such as Si and glass. So, the coating is usually deposited on Si or glass plates under the same preparation condition as that on the Mg alloy substrate for the subsequent SEM observation. This method can effectively simulate the coating structure of a relatively thick film on a metal substrate and has already been applied in the past years [20,29,30]. It is observed from Fig. 2(a) that this coating with three layers is about 1 μm thick. The top layer is the DLC film whose fracture is relatively smooth due to its amorphous microstructure. Fig. 2(b), (c) and (d) shows the surface morphology of the DLC/AlN/Al coating on the AZ31 magnesium alloy at three different magnifications. Apart from the occurrence of some micro-pores, most areas of the surface are very dense.

The microstructures and mechanical properties of magnesium alloys are prone to be influenced by temperature, so low temperature (just like the used deposition temperature in this study) must be applied in the deposition process of protective coatings. According to the literatures [31,32], the structure of vapor deposited coatings consists typically of a columnar growth structure and voided growth defects are easily formed due to atomic shadowing if the substrate temperature is low relative to the coating material melting point. Particularly when a significant oblique component is present in the coating flux, shadowing will induce open boundaries because high points on the growing surface receive more coating flux than valleys. In the process of film deposition, substrate surface roughness will promote this behavior with creating oblique deposition angles, which was also verified by Monte Carlo simulations [33,34]. Related to the coating deposition in our study (low deposition temperature and relatively rough substrate), it can be understood that through-thickness defects were inevitable in the prepared coating.

3.2. Anti-wear property

Fig. 3(a) and (b) shows the hardness and the elastic modulus of the samples as a function of displacement, respectively. In the measurement, the nano-indenter system worked at a Continuous Stiffness Measurement (CSM) mode. Surface smoothness of the sample is very important in this test because contact areas are calculated from the contact depth and area function rather than observed directly. But, the substrates prepared in this study were mechanically polished by hand, which also induced a poor quality of surface smoothness. Thus, as shown in Fig. 3, the standard deviation of the experimental data

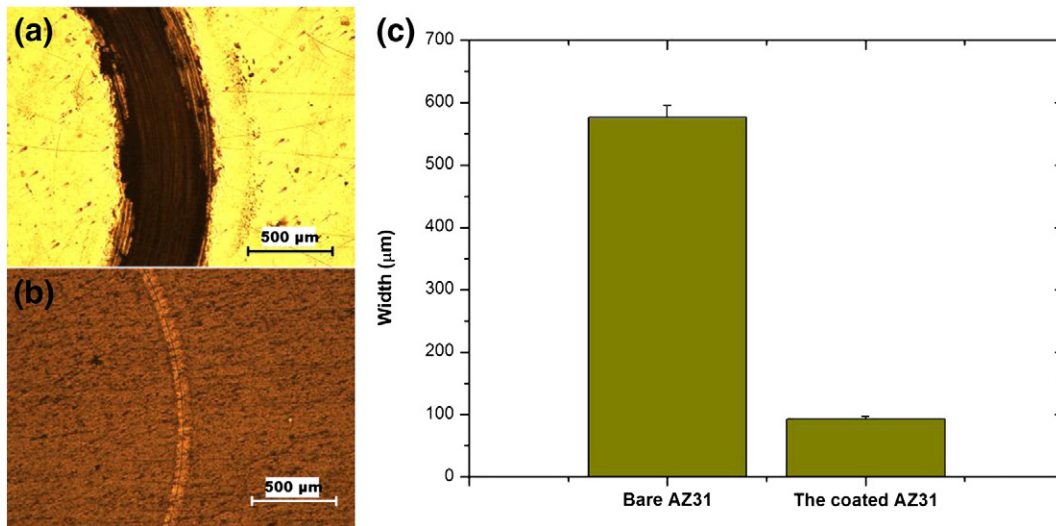


Fig. 5. (a) OM micrograph of the wear track of the bare AZ31 magnesium alloy, (b) OM micrograph of the wear track of the coated AZ31 magnesium alloy and (c) the statistical result of the wear track width.

was relatively high when the indentation depth was small. With the increase of indentation depth, the hardness of the coated sample was gradually decreased and finally tended to a stable value that represented the hardness of the Mg alloy substrate. The elastic modulus of the coated sample had a similar tendency as the hardness. In other words, it indicates that the surface mechanical property of the magnesium alloy was evidently improved by the DLC/AlN/Al coating.

Fig. 4 shows the relationship between the friction coefficient and the sliding distance. During the testing, the friction coefficient of the uncoated AZ31 was changing drastically while that of the coated AZ31 was very stable. It is found by calculation that the friction coefficient of the coated sample was greatly decreased from 0.36 to 0.10.

Fig. 5 shows the morphologies of the wear tracks after 30 m of sliding. The wear track of the coated AZ31 was much narrower than that

of bare AZ31. Fig. 5(c) gives the statistical result of the wear track width. The average wear track width of bare AZ31 was about 576.8 μm, whereas that of the coated AZ31 was only about 92.5 μm. The surface profiles of the wear tracks are shown in Fig. 6. The wear track of the coated AZ31 was obviously narrower and shallower than that of the bare AZ31. According to these above results, it can be concluded that the wear resistance of magnesium alloy after the surface treatment was greatly improved under the dry friction condition due to the formation of the protective coating with high hardness and low friction coefficient.

3.3. Anti-corrosion property

Fig. 7 shows the polarization curves of the bare AZ31 and the coated AZ31 in the 3.5 wt.% NaCl solution. It is observed that the curve

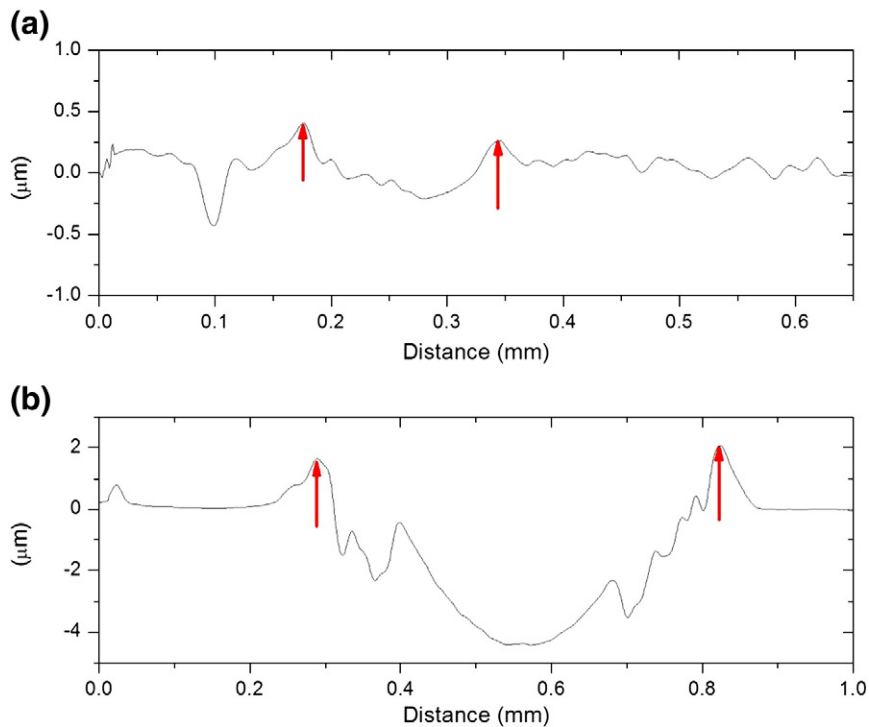


Fig. 6. Surface profiles of the wear tracks: (a) the coated AZ31 magnesium alloy and (b) bare AZ31 magnesium alloy.

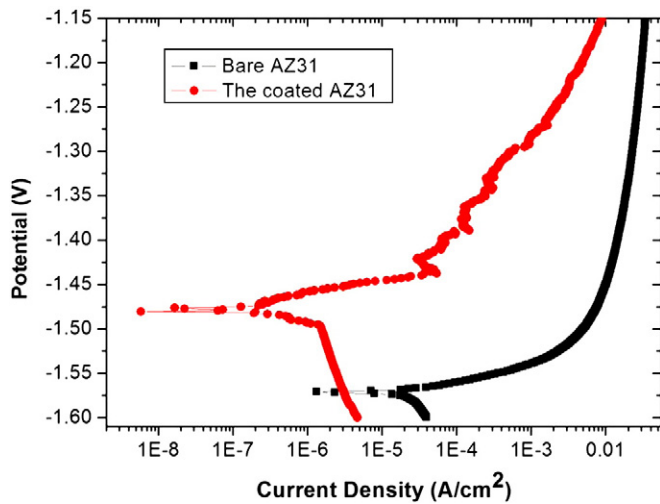


Fig. 7. Polarization curves of bare AZ31 and coated AZ31 in the 3.5 wt.% NaCl solution.

of the coated AZ31 shifted to the direction of lower current density and nobler corrosion potential. Generally, the cathodic polarization curve is assumed to represent the cathodic hydrogen evolution through water reduction, while the anodic curve represents the dissolution of the tested material [16]. Corrosion potential and corrosion current density can be derived directly from the region in the cathodic polarization curves by Tafel region extrapolation. According to the polarization curves shown in Fig. 7, it is deduced that the corrosion potential of the coated sample was increased from -1.57 V to -1.48 V and the corrosion current density of the coated sample was decreased from 2.25×10^{-5} A/cm² to 1.28×10^{-6} A/cm². The lower the corrosion current density is, the higher the corrosion resistance is. Therefore, it indicates that the corrosion resistance of the coated sample was improved in the 3.5 wt.% NaCl solution.

Fig. 8 shows the appearance of the samples after 6 h of immersion in the 3.5 wt.% NaCl solution. The surface of the bare AZ31 sample was badly corroded, whereas the coated AZ31 sample showed much less corrosion compared to the bare AZ31 sample. Simply based on the corroded areas, it confirms the conclusion of the polarization test. Furthermore, it is also found by comparison that some white

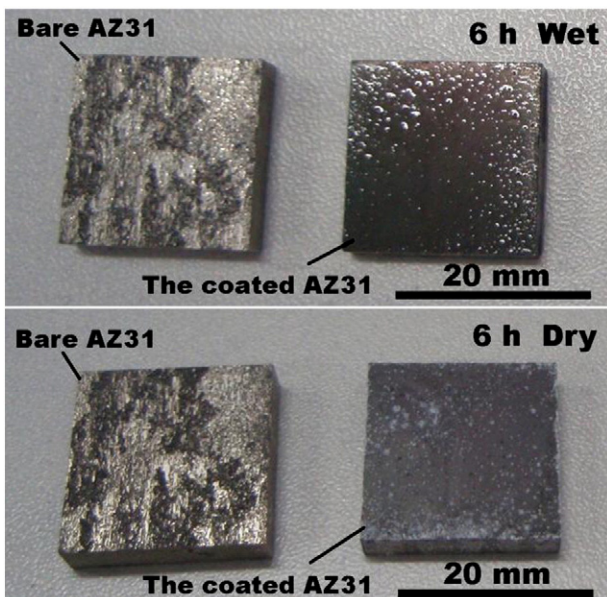


Fig. 8. Appearance of the samples after 6 h of immersion in the 3.5 wt.% NaCl solution.

corrosion products occurred on the dried surface of the coated sample. When the immersion test was finished, the samples were taken out from the NaCl solution and rinsed with deionized water. Initially, the surface of the coated sample was wet, so those corrosion products produced in the immersion test were immersed in the residual solution. As the surface was naturally dried, the corrosion products were separated out in the corrosion pits with the evaporation of water. In other words, those white regions were also the vestige of the local corrosion that happened in the immersion test.

In those previous studies, it has been understood that the through-thickness defects induce the pitting corrosion of the coated magnesium alloys in corrosive solutions. For example, Shi and Song [7–9] found that the corrosion failure of the ceramic-like anodized magnesium alloy with the porous microstructure was attributed to the pitting occurring at those through-thickness pores. Campo et al. [35] also discovered in their study that the failures of the thermally sprayed Al coatings on magnesium substrates were due to the presence of interconnected porosity. As depicted in the studies of Altun [20] and Hoche [2–4], it is nearly impossible to avoid the formation of pinholes in PVD coatings with current deposition techniques. Pores with dimensions of approximately 0.5 nm are almost always randomly distributed even in good quality PVD DLC films as described in the literatures [36,37]. From Fig. 2 (b) and (d), it can be seen that some micro-pores also existed on our prepared coatings. Therefore, through-thickness defects among them are the certain factor to induce the pitting corrosion of the coated magnesium alloy in the NaCl solutions in this study.

According to the phenomenon in the corrosion experiment, the following mechanism is introduced to explain the corrosion failure. First, the corrosive media penetrated the coating via those through-pores. When it got to the coating/substrate interface, galvanic cell was built between Al layer and Mg substrate. Then, the substrate as an anode in this cell began to dissolve with the reaction of hydrogen evolution. With the proceeding of the reaction, corrosion products piled up in the pores. But, according to the reports [38–40], the corrosion product of Mg alloys is porous (or loose) and soft. Therefore, its barrier effect to the corrosion reaction was very slight. Finally, the corrosion pits were enlarged, inducing the failure of the coating.

In addition, we also found that the corrosion current density in the anodic region of the coated AZ31 was much lower than that of bare AZ31. Because magnesium is the most active metal in the galvanic series, magnesium alloy component is always the active anode if it is in contact with other metals [41]. But, as the coated magnesium alloy contacts with other noble metals, the existence of the insulative DLC film can also reduce or eliminate the probability of the occurrence of galvanic corrosion. In this study, although both wear resistance and corrosion resistance of the magnesium alloy were enhanced, it is still a start of the designed fabrication of the protective system. More optimizations need to be performed in the future.

4. Conclusions

In summary, the DLC/AlN/Al coating was successfully deposited on the surface of AZ31 magnesium alloy by the combination of ion beam deposition and magnetron sputtering in this study. After the formation of the DLC/AlN/Al coating on magnesium alloy, the wear resistance of the magnesium alloy was greatly improved with the increase of the surface hardness and the decrease of the friction coefficient. In addition, the corrosion resistance of the coated magnesium alloy was also significantly improved in the 3.5 wt.% NaCl solution, but the multilayer coating could not prevent the occurrence of pitting corrosion due to the existence of through-thickness holes.

Acknowledgement

The authors would like to thank the financial support from the Outstanding Talent Recruiting Program dedicated to academician Q.J.

Xue, sponsored by Ningbo City, China (Grant No. 2009A31004), China Postdoctoral Science Foundation (Grant No. 20080430694), Shanghai Postdoctoral Scientific Program (Grant No. 08R214156) and Zhejiang Province Key Technologies R & D Program (Grant No. 2008C21055). The first author, Guosong Wu, would like to thank Prof. Feng Huang (NIMTE, Chinese Academy of Sciences) for his helpful discussion.

References

- [1] J.E. Gray, B. Luan, J. Alloys Compd. 336 (2002) 88.
- [2] H. Hoche, C. Rosenkranz, A. Delp, M.M. Lohrengel, Surf. Coat. Technol. 193 (2005) 178.
- [3] H. Hoche, C. Blawert, E. Broszeit, C. Berger, Surf. Coat. Technol. 193 (2005) 223.
- [4] H. Hoche, H. Scheerer, D. Probst, E. Broszeit, C. Berger, Surf. Coat. Technol. 174–175 (2003) 1018.
- [5] F. Hollstein, R. Wiedemann, J. Scholz, Surf. Coat. Technol. 162 (2003) 261.
- [6] G. Wu, X. Wang, K. Ding, Y. Zhou, X. Zeng, Mater. Charact. 60 (2009) 803.
- [7] Z. Shi, G. Song, A. Atrens, Corros. Sci. 47 (2005) 2760.
- [8] Z. Shi, G. Song, A. Atrens, Corros. Sci. 48 (2006) 3531.
- [9] Z. Shi, G. Song, A. Atrens, Surf. Coat. Technol. 201 (2006) 492.
- [10] J. Robertson, Mat. Sci. Eng. R 37 (2002) 129.
- [11] N. Yamauchi, N. Ueda, A. Okamoto, Surf. Coat. Technol. 201 (2007) 4913.
- [12] N. Yamauchi, K. Demizu, N. Ueda, Thin Solid Films 506–507 (2006) 378.
- [13] J. Choi, J. Kim, S. Nakao, Nucl. Instrum. Methods. B 257 (2007) 718.
- [14] J. Choi, S. Nakao, J. Kim, Diamond Relat. Mater. 16 (2007) 1361.
- [15] M. Xu, L. Li, Y. Liu, X. Cai, Q. Chen, P.K. Chu, Surf. Coat. Technol. 201 (2007) 6707.
- [16] G. Wu, L. Sun, W. Dai, L. Song, A. Wang, Surf. Coat. Technol. 204 (2010) 2193.
- [17] J. Zhang, W. Zhang, C. Yan, K. Du, F. Wang, Electrochim. Acta 55 (2009) 560.
- [18] A. Pardo, P. Casajus, M. Mohedano, A.E. Coy, F. Viejo, Appl. Surf. Sci. 255 (2009) 6968.
- [19] G. Wu, X. Zeng, G. Yuan, Mater. Lett. 62 (2008) 4325.
- [20] H. Altun, S. Sen, Surf. Coat. Technol. 197 (2005) 193.
- [21] W. Dai, H. Zheng, G. Wu, A. Wang, Vacuum doi:10.1016/j.vacuum.2010.06.001.
- [22] Y. Taki, O. Takai, Thin Solid Films 316 (1998) 45.
- [23] J. Wu, C. Chen, C. Shin, M. Li, M. Leu, A. Li, Thin Solid Films 517 (2008) 1141.
- [24] A.C. Ferrari, Diamond Relat. Mater. 11 (2002) 1053.
- [25] H. Cheng, Y. Sun, J.X. Zhang, Y.B. Zhang, S. Yuan, P. Hing, J. Cryst. Growth 254 (2003) 46.
- [26] H. Cheng, Y. Sun, P. Hing, Surf. Coat. Technol. 166 (2003) 231.
- [27] E. Valcheva, S. Dimitrov, D. Manova, S. Mändl, Surf. Coat. Technol. 202 (2008) 2319.
- [28] H.C. Barshilia, B. Deepthi, K.S. Rajam, Thin Solid Films 516 (2008) 4168.
- [29] G. Wu, X. Zeng, G. Li, S. Yao, X. Wang, Mater. Lett. 60 (2006) 674.
- [30] G. Wu, Mater. Lett. 61 (2007) 3815.
- [31] J.A. Thornton, J. Vac. Sci. Technol. A 4 (1986) 3059.
- [32] L.A. Zepeda-Ruiz, G.H. Gilmer, C.C. Walton, J. Cryst. Growth 312 (2010) 1183.
- [33] M. Yoshiya, K. Wada, B.K. Jang, H. Matsubara, Surf. Coat. Technol. 187 (2004) 399.
- [34] Y. Kaneko, Y. Hiwatari, K. Ohara, T. Murakami, Surf. Coat. Technol. 169–170 (2003) 215.
- [35] M. Campo, M. Carboneras, M.D. López, B. Torres, Surf. Coat. Technol. 203 (2009) 3224.
- [36] A. Zeng, E. Liu, I.F. Annergren, S.N. Tan, S. Zhang, Diamond Relat. Mater. 11 (2002) 160.
- [37] V. Novotny, N. Staud, J. Electrochem. Soc. Electrochem. Sci. Technol. 135 (1988) 2931.
- [38] X. Guo, J. Chang, S. He, W. Ding, X. Wang, Electrochim. Acta 52 (2007) 2570.
- [39] G. Wu, W. Dai, L. Song, A. Wang, Mater. Lett. 64 (2010) 475.
- [40] J. Chang, P. Fu, X. Guo, L. Peng, W. Ding, Corros. Sci. 49 (2007) 2612.
- [41] G. Song, B. Johannesson, S. Hapugoda, D. StJohn, Corros. Sci. 46 (2004) 955.